

When Does a Camera See Rain?*

Kshitiz Garg and Shree K. Nayar
Department of Computer Science, Columbia University
New York, New York 10027
Email: {kshitiz,nayar}@cs.columbia.edu

Abstract

Rain produces sharp intensity fluctuations in images and videos, which degrade the performance of outdoor vision systems. These intensity fluctuations depend on various factors, such as the camera parameters, the properties of rain, and the brightness of the scene. We show that the properties of rain – its small drop size, high velocity, and low density – make its visibility strongly dependent on camera parameters such as exposure time and depth of field. We show that these parameters can be selected so as to reduce or even remove the effects of rain without altering the appearance of the scene. Conversely, the parameters of a camera can also be set to enhance the visual effects of rain. This can be used to develop an inexpensive and portable camera-based rain gauge that provides instantaneous rain rate measurements. The proposed methods serve to make vision algorithms more robust to rain without any necessity for post-processing. In addition, they can be used to control the visual effects of rain during the filming of movies.

1 Dynamic Weather And Vision

Most algorithms used in outdoor vision systems assume that image intensities are proportional to scene brightness. However, dynamic weather (rain and snow) introduces sharp intensity fluctuations in images and videos, violating this basic assumption. Figure 1(a) shows an example of the complex intensity patterns produced by rain. As a result, rain can severely degrade the performance of a wide range of outdoor vision algorithms, including, feature detection, stereo correspondence, tracking, segmentation, and object recognition.

While various algorithms [10, 9, 13, 11] for handling the visual effects of steady weather (fog, mist and haze) have been developed, little work has been done on the effects of dynamic weather. Recently, Garg and Nayar [1] proposed a post-processing algorithm to detect and remove rain from a video that has already been acquired. This technique is also useful in cases where we have no control over camera parameters during video capture. However, in many outdoor vision settings we do have control over these parameters. In this work we show that by appropriately selecting camera parameters one can reduce (and sometimes remove) the effects of rain, without appreciably altering the appearance of the scene. Note that this is done during image acquisition and does not require any

*This work is funded in part by the National Science Foundation, Award No. IIS-04-12759 and by the Office of Naval Research, Award No. N00014-05-1-0188.

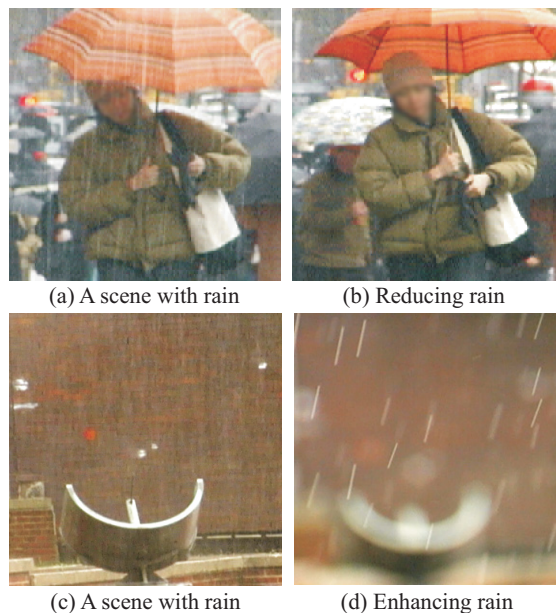


Figure 1: Camera parameters and the visibility of rain. (a) An image of a scene taken under rain with default camera parameters. The sharp intensities produced by rain severely degrade the performance of vision algorithms. (b) An image of the same scene taken with a different set of camera parameters reduces the visual effects of rain at the time of image acquisition, without noticeably altering the appearance of the scene. The person's face has been blurred. (c) A scene in rain. (d) Camera parameters can also be set to amplify the visual effects of rain. This can be used to develop a camera-based rain gauge.

post-processing. The following are the key contributions of our work:

Analysis of Visibility of Rain: We analyze the various factors, such as properties of rain, camera parameters, and scene brightness, that affect the appearance of rain in videos. We have derived analytical expressions for these dependencies. We show that the visibility of rain increases as the square of the raindrop size. Rain visibility also decreases linearly with the brightness of the background scene. Most importantly, we show that the high velocity and small size of raindrops make rain visibility strongly dependent on camera parameters, such as exposure time and depth of field¹. We have conducted extensive experiments that verify our analytical models.

¹In contrast, the appearance of snow does not depend strongly on camera parameters due to the slow velocity and large size of its particles.

Camera Parameters for Removal of Rain: Based on the above analysis, we present a method that sets the camera parameters to remove/reduce the effects of rain without altering the appearance of the scene. This is possible because, given the finite resolution and sensitivity of the camera, a wide range of camera settings (exposure time, F-number, focus setting) produce essentially the same scene appearance. However, within this range the appearance of rain can vary significantly. Figure 1(a) shows an image from a video of a person walking in rain. Figure 1(b) shows an image of the same scene (with the same lighting, rain, etc.) with a different camera setting to greatly reduce the visibility of rain. Note that this approach does not require any post-processing and can be easily incorporated as a feature into consumer cameras. We present several experimental results that show our approach to be very effective in a wide range of scenarios. In the extreme cases of very heavy rain or fast moving objects that are close to the camera, our approach is not as effective. In such cases, however, a post-processing method like the one in [1] can be used.

Camera Based Rain Gauge: Camera parameters can also be set to *enhance* the visual effects of rain, as shown in Figure 1(c-d). This can be used to build a camera-based rain gauge that measures rain rate. A major advantage of a camera-based rain gauge over a conventional one is that it can provide measurements on a much finer time scale. While specialized instruments such as the disdrometer [12, 6] can also provide rain measurements at a fine time scale, they are very expensive and are not portable. On the other hand, a vision based rain gauge is cheap and portable.

The paper is structured as follows. We begin by defining the notion of rain visibility. We then derive the models that relate rain visibility to camera parameters. The effectiveness of our approach is then demonstrated using several examples. Finally, we present the camera-based rain gauge and related experiments.

2 Visibility of Rain

Rain consists of a large number of drops falling at high speed. These drops produce high frequency spatio-temporal intensity fluctuations in videos. In this section, we derive an analytical expression that relates the visibility of rain to the camera parameters, the properties of rain, and the scene brightness. For the purpose of analysis we have assumed a static background. Later we show how the analysis can be used for the general case of dynamic scenes.

Figure 2(a) shows a frame from a video of a static scene taken in rain, where the effects of rain are visible. The plot below shows the intensity fluctuations produced by rain at a pixel, which is characterized by large variance over time. A frame from a video of the same scene (under identical environmental conditions) taken with camera parameters set to reduce the visual effects of rain is shown in Figure 2(b). Here, the effects of rain are not visible. The variation in intensity at the same pixel is now low. Hence, variance at a pixel over time can be used

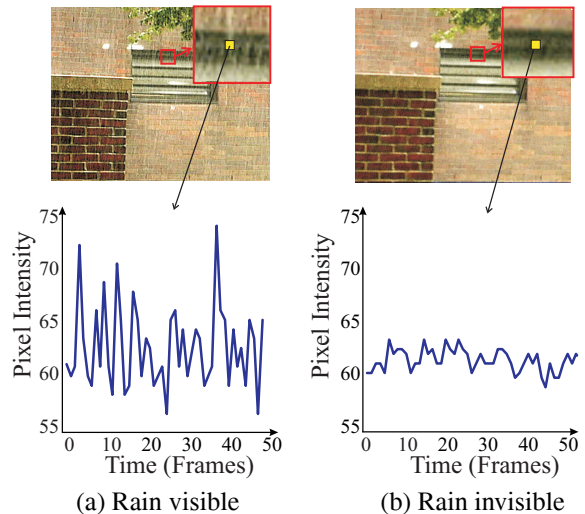


Figure 2: Dynamic weather and visibility: (a) Frame from a video of a scene taken in rain. Rain produces sharp intensity variations at a pixel, which result in a signal with large variance over time. (b) Frame from a video of the same scene taken with a different set of camera parameters. The effects of rain are not visible. The intensity at the same pixel shows low variance over time.

to measure the visibility of rain and can therefore be used as a quantitative measure of it. We now derive how variance (visibility) is related to the various factors mentioned above. To do this we will first model the intensities produced by individual raindrops and then consider the effects due to a volume of rain.

2.1 Camera and Intensity of a Raindrop

Raindrops fall at high velocities relative to the exposure time of the camera, producing severely motion-blurred streaks in images. Also, due to the limited depth of field of a typical camera, the visibility of rain is significantly affected by defocus. In this section we model the motion-blurred and the defocused intensities produced by raindrops. These intensities are later used to derive the effects due to a volume of rain.

For deriving these intensities we assume the camera to have a linear radiometric response. The intensity I at a pixel is related to the radiance L as [5],

$$I = k \frac{\pi}{4} \frac{1}{N^2} T L, \quad (1)$$

where, k is the camera gain, N is the F-number, and T is the exposure time. The gain can be adjusted so that image intensities do not depend on specific N and T settings. This implies that k should change such that k_0 is constant, where,

$$k_0 = k \frac{\pi}{4} \frac{T}{N^2}. \quad (2)$$

Therefore, the image intensity can be written as $I = k_0 L$. We now model the change in intensities produced by rain streaks.

Raindrops and Exposure Time: Figure 3(a) shows a pixel looking at raindrops that lie at different distances, z , from the camera. Drops close to the camera ($z < z_m$) project to a size larger than a pixel, where $z_m = 2fa$ (a is the radius of the

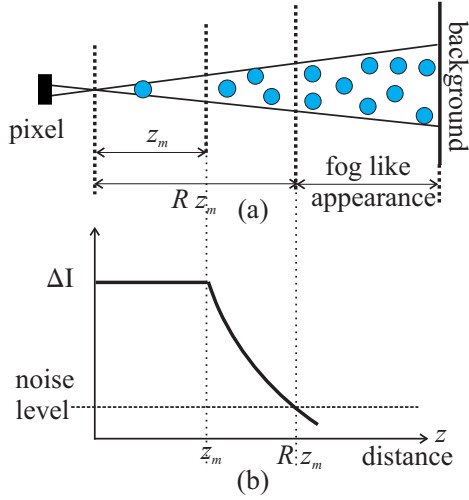


Figure 3: The change in intensity produced by a falling raindrop as a function of the drop’s distance z from the camera. The change in intensity ΔI does not depend on z for drops that are close to the camera ($z < z_m$). While for raindrops far from the camera ($z > z_m$), ΔI decreases as $1/z$ and for distances greater than Rz_m , ΔI is too small to be detected by the camera. Therefore, the visual effects of rain are only due to raindrops that lie close to the camera ($z < Rz_m$) which we refer to as the *rain visible region*.

drop and f is the focal length in pixels). The change in intensity ΔI produced by these drops is given by [1]

$$\Delta I = I_r - I_b = k_0 \frac{\tau}{T} (L_r - L_b), \quad (3)$$

where, I_r is the motion-blurred intensity at a pixel affected by rain, and $I_b = k_0 L_b$ is the intensity at a pixel not affected by rain (that is the background intensity). L_r and L_b are the brightnesses of the raindrop and the background, respectively, and T is the exposure time of the camera. $\tau \simeq 2a/v$ is the time that a drop stays within the field of view of a pixel and v is the drop’s fall velocity. From the above equation we see that change in intensity produced by drops in region $z < z_m$ decreases as $1/T$ with exposure time and does not depend on z .

On the other hand, the change in intensity produced by drops far from camera that is $z > z_m$ is given by (see appendix for derivation)

$$\Delta I = k_0 \frac{4f a^2}{z v} \frac{1}{T} (L_r - L_b). \quad (4)$$

As in the previous case ΔI decreases inversely with exposure time. However, now ΔI also depends on the drop’s distance from the camera, and decreases as $1/z$.

Figure 3(b) illustrates how the change in intensity ΔI produced by a falling raindrop is related to its distance from the camera. The change in intensity is almost constant for distances less than $z_m = 2fa$. For $z > z_m$ the intensity fluctuation decreases as $1/z$ and for distances greater than Rz_m (where R is a constant), the fluctuation ΔI becomes too small to be detected by a camera². Hence, the visual effects of rain are only

²Drops in the region $z > Rz_m$ only produce aggregate scattering effects

produced by raindrops in the region $z < Rz_m$. We refer to this region ($0 < z < Rz_m$) as the *rain visible region*. The value of R depends on the brightness of the scene and camera sensitivity. For the Canon XL1 video camera we empirically found the value of R to be approximately 3. Thus, when the field of view is 10° (focal length ≈ 4000 pixels), Rz_m is around 24m assuming $a = 1\text{mm}$ as the average drop size.

Rain and Depth of Field: We now analyze the effects of a limited depth of field on the intensity produced by raindrops. We can approximate defocus as a spreading of change in intensity produced by a focused streak uniformly over the area of a defocused streak³. Hence, the change in intensity ΔI_d due to a defocused drop is related to the change in intensity ΔI of a focused streak as

$$\Delta I_d = \frac{A}{A^d} \Delta I = \frac{w(v_i T)}{(w + b_c)(v_i T + b_c)} \Delta I, \quad (5)$$

where, A and A^d are the areas of the focused and the defocused rain streak, respectively, w is the width of the focused drop in pixels, b_c is the diameter of the defocus kernel (blur circle) [5], v_i is the image velocity of the drop, and T is the exposure time of the camera. Since raindrops fall at high velocity we can assume that $v_i T \gg b_c$. Hence, the above expression simplifies to

$$\Delta I_d = \frac{w}{w + b_c} \Delta I. \quad (6)$$

Substituting ΔI from equation (3) we get the change in intensity due to a defocused drop that lies close to the camera ($z < z_m$) as

$$\Delta I_d = \frac{w}{w + b_c} \frac{\tau}{T} (L_r - L_b). \quad (7)$$

The change in intensity due to a defocused drop that lies in the region $z > z_m$ is obtained by substituting⁴ $w = 1$ and ΔI from equation (4) in equation (6),

$$\Delta I_d = \frac{1}{b_c + 1} \frac{f a^2}{z v} \frac{1}{T} (L_r - L_b). \quad (8)$$

Equations (7) and (8) give us the intensity change produced by a defocused and motion-blurred raindrop. We now use them to find the variance at a pixel produced by a volume of rain.

2.2 Camera Parameters and Volume of Rain

Consider a camera looking at a distribution of raindrops in a volume, as shown in Figure 4. This distribution of falling drops in 3D maps to the 2D image plane via perspective projection. As a result, multiple drops at different depths may project to the same pixel during the exposure time of the camera, producing intensity variations much larger than those of individual drops. To model these volumetric effects, we partition the

similar to fog – no dynamic effects are visible.

³Exact modeling of defocus is required to obtain intensity variations across a rain streak. However, since rain streaks are only a few pixels wide, the intensity variation across a rain streak is not significant and can be neglected.

⁴The fact that the projected drops only occupy a portion of the pixel is already taken into account in computing ΔI in equation (4).

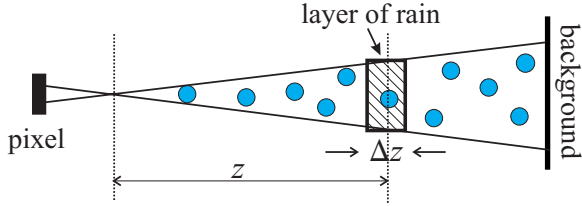


Figure 4: Intensity fluctuations produced by a volume of rain. To model the volumetric effects we partition the volume into thin layers. The intensity properties of the layers are then summed to obtain the total effect due to a volume.

volume into thin layers of rain of thickness Δz , as shown in Figure 4. We first compute the variance due to a single layer of rain. The variance due to a volume of rain is then the sum of the variances due to the different layers. In the appendix, we have shown that variance $\sigma_r^2(I, z)$ due to a single layer of rain at distance z is given by

$$\sigma_r^2(I, z) = \bar{n}(z) w^d(z) \Delta I_d^2(z), \quad (9)$$

where, $\bar{n}(z)$ is the mean number of drops in the layer that pass through a pixel's field of view during the exposure time of the camera and is given by equation (16), $w^d(z) = w(z) + b_c(z)$ is the width of the defocused streak due to a raindrop at depth z , and $\Delta I_d(z)$ is the change in intensity produced by it (see equations (7) and (8)). Substituting the values of \bar{n} , w^d and ΔI_d we get the variance $\sigma_r^2(I, z)$ due to a layer of rain as

$$\sigma_r^2(I, z) dz = k_0^2 \frac{4 a^4 \rho (L_r - L_b)^2}{v T} \frac{f dz}{z (w(z) + |b_c(z)|)}, \quad (10)$$

where, a is the size of the drop, ρ is the drop size density, v is the velocity of the drop and $w(z) = \max(\frac{fz}{a}, 1)$.

Since layers are non-overlapping and independent, the variance $\sigma_r^2(I, z)$ due to different layers can be added to find the variance due to a volume of rain. Substituting for $w(z)$, $b_c(z)$, and integrating the above equation over z , we obtain the variance and hence the standard deviation $\sigma_r(I)$ due to a volume of rain as,

$$\sigma_r(I) = \frac{k_0}{\sqrt{T}} \frac{a^2 \sqrt{\rho}}{\sqrt{v(a)}} (L_r - L_b) \sqrt{\mathcal{G}(f, N, z_0)}, \quad (11)$$

where, $\mathcal{G}(f, N, z_0)$ is a function (see appendix for exact form) of focal length f , F-number N , and the distance z_0 of the focus plane. Equation (11) shows that the variance of rain increases as the square of the size a of the raindrop. The visibility of rain also increases with density ρ of rain. It also shows that the standard deviation σ_r due to rain decreases linearly with background brightness L_b .

We now look at the dependence of the visibility of rain (i.e. σ_r) on camera parameters, as is shown in Figure 5(a-c). Figure 5(a) shows that the visibility of rain decreases as $1/\sqrt{T}$ with exposure time of the camera. Figure 5(b) shows that σ_r initially increases rapidly with F-number N and then reaches

saturation for higher F-numbers. Figure 5(c) shows the σ_r dependence with respect to distance z_0 of the focal plane. The curve shows a maximum at the location of the focus plane that keeps the largest possible region of rain in focus.

We conducted experiments to verify these dependencies on camera parameters. A Canon XL1 camera was used in our experiments. The camera was calibrated to make its radiometric response linear⁵. The standard deviation σ_r for a given camera setting was computed by taking videos of rain (200 frames) against a stationary background of uniform brightness. 1800 pixels⁶ were used to estimate the variance. The red marks in Figure 5(a-c) show the mean values of the measured σ_r and error bars show the uncertainty in the measurement of σ_r . The measured variances are in close agreement with the values predicted by our model. For details regarding the camera settings for specific experiments please see the caption of Figure 5. These experiments validate the correctness of the derived analytical model. We next demonstrate some useful applications that are based on our models.

3 Camera Parameters for Rain Removal

Until now we have looked at the effects of camera parameters on rain visibility with the assumption that the scene is static. We now show how this analysis can be used to reduce the effects of rain in the case of dynamic scenes. Although changing camera parameters may affect scene appearance, in typical scenes, there is some flexibility in setting camera parameters. We use this flexibility to remove rain without affecting scene appearance. We present some common scenarios where rain produces strong effects and offer techniques to reduce them. Please see videos at www.cs.columbia.edu/CAVE. All the experiments were done with a radiometrically calibrated Canon XL1 camera. The camera gain was set on the automatic mode to maintain the average brightness of the scene constant over different camera settings.

Reducing Rain using Depth of Field: Figure 6I(a) shows a frame from a traffic scene video. Since the scene has fast moving objects, a short exposure time $T = 8\text{ms}$ is required, which increases the degradation due to rain. However, the scene is far from the camera and has small depth variations. Our analysis shows that for such types of scenes the visibility of rain can be reduced by a factor of 0.4944 (equation (11)) by decreasing the F-number from its default value of $N = 12$ to $N = 2.4$. Figure 6I(b) shows a frame from a video of the same scene taken with F-number $N = 2.4$. Note that rain effects are significantly reduced (see the magnified image regions that are shown in full resolution) while scene appearance has not changed. The measured reduction in rain visibility (σ_r) due to the change in

⁵We also compute the noise properties of the camera. For a stationary scene the total variance at a pixel is the sum of rain and camera noise. Since camera noise is independent of rain noise, the variance due to rain can be obtained by subtracting variance due to camera noise.

⁶Rain produces directional correlation in videos. Hence, to ensure that variance estimates are from independent pixels we selected 60×30 pixels from a uniform brightness patch that were separated by 5 pixels in horizontal direction and 10 pixels in vertical direction.

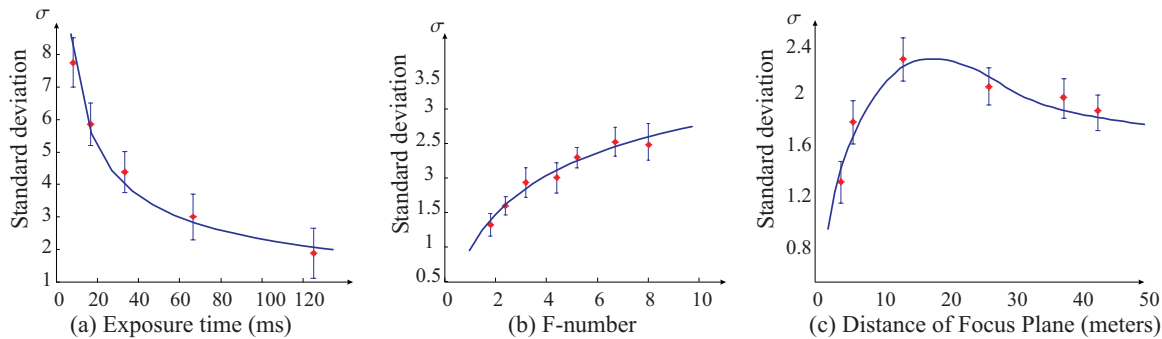


Figure 5: Experimental verification of the analytical model that relates visibility of rain σ_r to camera parameters. The solid curves show σ_r as given by equation (11). The red marks show the mean values of the measured σ_r and the error bars show the uncertainty in measurement. (a) σ_r as a function of exposure time T . Other camera parameters were set to focal length $f = 3155$ pixels, F-number $N = 5.6$, and distance of focused plane $z_0 = 10$ m. The exposure time was varied from 8ms to 125ms. The experiments verify the $1/\sqrt{T}$ dependence on exposure time. (b) The visibility dependence on aperture size (F-number). The F-number was increased from 1.8 to 8. Other camera parameters were fixed to $f = 8000$ pixels, $T = 16$ ms and $z_0 = 14$ m. (c) Dependence of visibility on distance of the focal plane z_0 . The focal plane was kept at different distances from the camera from $z_0 = 4$ m to $z_0 = 40$ m. Other camera parameters were fixed at $f = 8000$ pixels, $T = 16$ ms, $N = 6.7$. In all the above cases the experimental values show close agreement with the values predicted by our models.

F-number is 0.4541 (error margin=0.0884), which is close to the predicted value of 0.4944.

Reducing Rain using Exposure Time: Figure 6II(a) shows a frame from a video of people walking on a sidewalk. Unlike the previous example, this scene has slow motion (less than 15 pixels/sec). However, the scene is close to the camera (lies in the rain visible region $z < Rz_m$) and has a large depth range, hence a large F-number $N = 14$ is needed to capture this scene. The effects of rain are strong in such a scenario, as can be seen in Figure 6II(a). For this type of scene our analysis suggests that the visibility of rain can be reduced by a factor of 0.5 (obtained from equation (11)) by increasing the exposure time from the default value of 16ms to 66ms. As can be seen in Figure 6II(b), the visual effects of rain are almost removed without affecting the scene appearance. The measured reduction in rain visibility is 0.4615 (error margin 0.0818), which is close to the predicted value of 0.5.

Reducing Rain using Multiple Parameters: Figure 6(III)(a) shows a scene with moderate depth variation and motion taken with default camera parameters – exposure time $T = 16$ ms and F-number $N = 12$. For such scenarios the visibility of rain can be significantly reduced by increasing the exposure time to $T = 33$ ms and decreasing the F-number to $N = 6$. Figure 6III(b) shows a frame from a video taken with these camera settings. The effects of rain are significantly reduced. The measured reduction in rain visibility is 0.5496 (error margin 0.094), which is close to the predicted value of 0.4944.

Reducing Heavy Rain: Figure 6(IV)(a) shows a frame from a video of a scene in heavy rain taken with default camera parameters – exposure time $T = 16$ ms and F-number $N = 4$. The visual effects of rain are very strong. Even in this case we can significantly reduce the effects of rain by setting exposure time to 120ms as seen in Figure 6IV(b). The measured reduction in rain visibility is 0.3763 (error margin 0.0824) which is close to the predicted value of $\sigma_r = 0.3536$.

These experiments demonstrate the effectiveness of reducing rain by setting appropriate camera parameters. This technique provides a simple and practical method to reduce rain in videos without any need for post-processing and can be easily incorporated as a feature into consumer cameras. As an example, in Table 1 we show the camera parameters for the Canon XL1 that should be used to reduce the visual effects of rain for various types of scenes. Only a coarse estimation of scene properties is needed. We categorize scene distances into *close* and *far*, depending on whether the distance of the scene from the camera is less than Rz_m or not. For the Canon XL1, when the field of view is 10° , Rz_m is approximately 24m.

Similarly, we need a coarse estimate for scene motion. Objects with image velocities less than 15 pixels/sec are considered slow, i.e., no motion-blur is observed if the exposure time is set

Scene Motion	Near Distance	Depth Range	Exposure Time ms	F-number
(a) slow	close	large	66	14
(b) slow	close	small	33	4.4
(c) slow	far	large	66	6
(d) slow	far	small	33	2
(e) fast	close	large	X	X
(f) fast	close	small	X	X
(g) fast	far	large	8	6
(h) fast	far	small	8	2.4

Table 1: This table shows how our results can be incorporated as a feature into commercial video cameras to reduce the effects of rain. The camera parameters given here are for the Canon XL1 video camera. The scene is described using coarse estimate of the scene properties – motion (image velocities), near distance, and its depth range. These scene properties can be manually set by the user or estimated automatically by the camera itself. Once the scene properties are determined, using a lookup table similar to this one, camera parameters can be set to reduce rain. The cases (e) and (f) refer to cases where it is not possible to remove rain without affecting the scene appearance. Cases (a) and (h) correspond to the scenarios shown in Figure 6 (II) and (I), respectively.

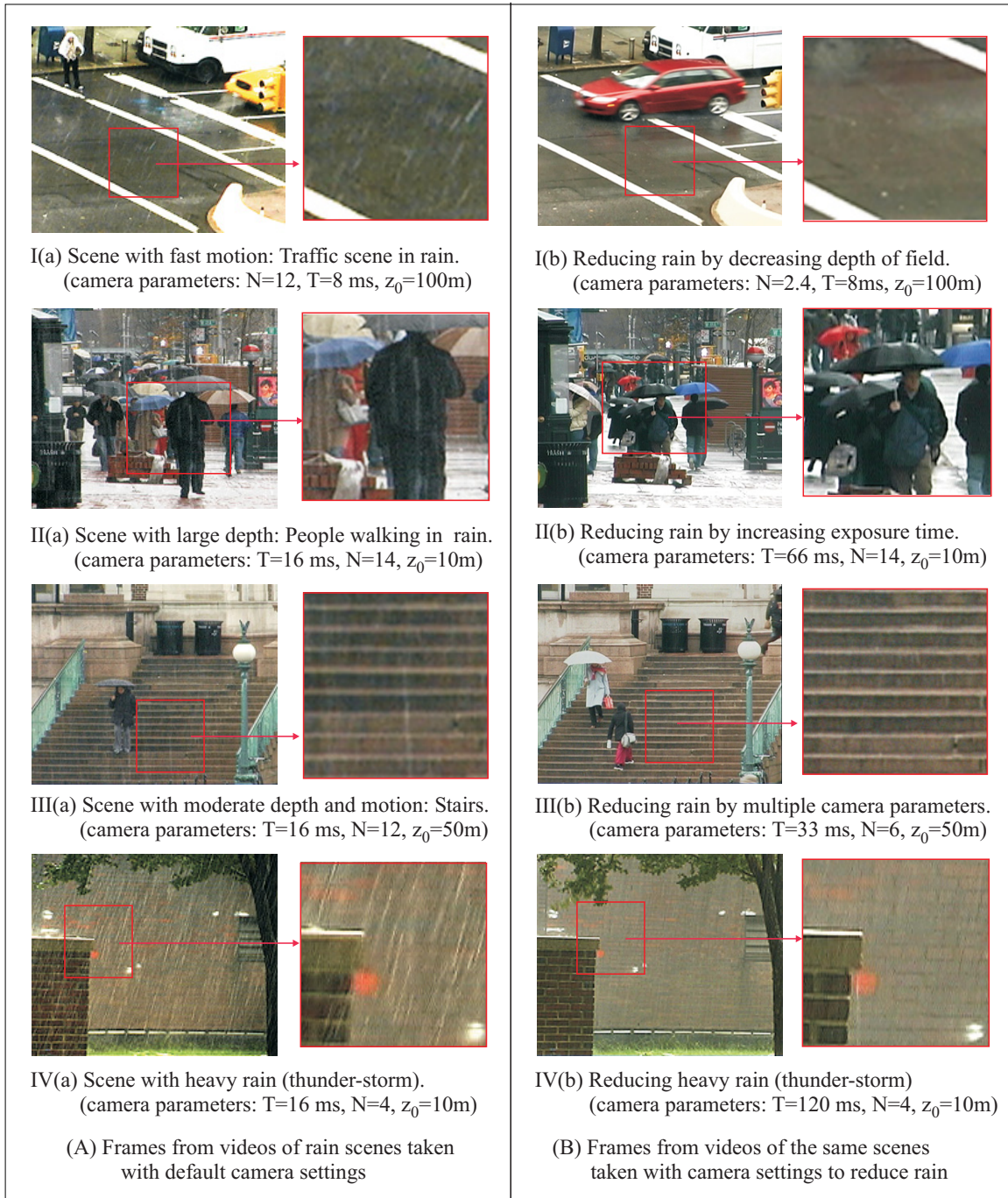


Figure 6: Some common scenarios where rain produces strong effects and our results on rain reduction/removal. The frames in column (A) show the scene captured with default camera parameters (camera parameters set automatically by the camera for a given scene). The frames in column (B) show the same scene (with identical environmental conditions) taken with camera parameters estimated by our method to reduce rain visibility. (I)(a) A traffic scene in rain. The scene has fast motion and low depth variation. Our analysis shows that rain can be reduced in this scene by decreasing the F-number to $N = 2.4$ as shown in I(b). (II) (a) Frame from a video of people walking on a sidewalk. The scene has a large depth range and slow moving objects. For this scene the visibility of rain can be reduced by increasing the exposure time to $T = 66$ ms as shown in II(b). (III)(a) An image from a video of people walking on stairs. The scene has moderate depth range and motion. Our analysis shows that to reduce rain in this scene without modifying scene appearance, both the exposure time and F-number need to be changed to $T = 33$ ms and $N = 6$, respectively.(IV) (a) A frame from a video of a scene with heavy rain. Even in this extreme case of very heavy rain, we can reduce rain visibility significantly by increasing the exposure time to $T = 120$ ms as shown in IV(b). Note that in all these cases the effects of rain were reduced during image acquisition and no post-processing was needed. Also, the visual effects of rain were reduced without affecting the scene appearance. Please see videos at www.cs.columbia.edu/CAVE.



(a) Light rain (b) Moderate rain (c) Heavy rain

Figure 7: Frames from a camera-based rain gauge for different types of rainfall (a) Light rain. (b) Moderate rain (c) Heavy rain. The results of rain rate measurements are given in Table 2.

to 1/15 of a second or higher. Depth ranges greater than Rz_m are considered large. This method, however will not be able to reduce rain in scenes with very fast motion and when objects are very close to the camera, cases that correspond to rows (e-f) in Table 1. Increasing the exposure time or decreasing the depth of field in such scenes might not be possible without affecting the scene appearance. In such cases postprocessing techniques [1] might be required to remove the effects of rain.

4 Camera Based Rain Gauge

We now show how the visual effects of rain can be enhanced to develop a camera-based rain gauge – a device that measures rain rate. The vision-based rain gauge provides instantaneous rain rate measurements (time scale of seconds) and is robust to camera and background scene motion.

Our rain gauge measures rain rate by observing the size and the number of drops in a small volume of rain over time. This volume is defined by the F-number and the distance of the focal plane z_0 . Since we want a small depth of field, the F-number is set to a low value. The value of z_0 is set so that the smallest raindrops are also visible, that is $z_0 \leq 2fa_{min}$, where f is the focal length and $a_{min} = 0.5\text{mm}$ is the radius of the smallest raindrop [8]. As z_0 is known, we can then determine the size and velocity of the raindrops from the focused rain streaks. A smaller exposure time also enhances the visibility of rain streaks.

Each frame is segmented into rain and non-rain regions using the method described in [1]. A linear time sequential labeling algorithm [5] is then used to obtain the number of raindrops, size, and velocity (length of streaks) of each drop. Defocused streaks are removed by rejecting rain streaks that do not satisfy the velocity-size relationship of raindrops given by [3]⁷,

$$v(a) = 200\sqrt{a}, \quad (12)$$

where, a is the radius of the drop. Each frame gives a count of the number of drops of a specific size in the observed rain volume. Repeating this over several frames provides a robust estimate of the number of drops of different sizes and hence the density $\rho(a)$ of rain. The total rain rate h can then be computed from the estimated $\rho(a)$ using [14],

$$h = \int h(a)da = 3.6 * 10^6 \frac{4\pi}{3} \int a^3 \rho(a) v(a) da. \quad (13)$$

⁷Defocus primarily affects the width of the streaks, resulting in an over-estimated size of raindrops. On the other hand, defocus does not affect the estimate of velocity significantly. As a result, the size and the velocity relation given by equation (12) is not satisfied by defocused drops.

Type of Rainfall	Camera parameters (f, N, z_0, T)	Measured Rain rate mm/hr	Reported Rain rate mm/hr
(a) Light	(7095, 3.8, 3, 16)	1.34	0.763
(b) Moderate	(5148, 4.4, 3, 4)	3.215	2.28
(c) Heavy	(3300, 1.8, 3, 4)	14.28	11.17

Table 2: A comparison of rain rate measured by the camera-based rain gauge to the reported hourly rain rate obtained from the National Climatic Data Center (NCDC). Here, f is the focal length in pixels, N is the F-number, z_0 is the distance of the focus plane in meters, and T is the exposure time in milliseconds. The differences in rain rate measurements are expected due to the distance of few miles between measuring locations and differences in time scale, (seconds vs hours) at which rain rates are measured.

We conducted a number of experiments to verify the accuracy of our camera based rain gauge. Figure 7 shows frames from three illustrative scenarios. Figure 7(a) shows mild rain, Figure 7(b) shows moderate rain, and Figure 7(c) shows heavy rain. We computed the rain rates for these events over a short duration of 10s. The camera parameters were set to enhance the effects of rain and the rain rate measurements obtained are given in Table 2. The results are compared with the reported rain rates from the National Climatic Data Center (NCDC). The differences in the measured and the observed rain rates are expected, since the measurement locations were a few miles apart. Also, the rain rate estimates obtained from the camera-based gauge are for a short time duration of 10s while rain rates obtained from NCDC are averaged over a period of one hour. Moreover, conventional rain gauges tend to report low rain rates due to splashing and wind effects [4].

5 Conclusion

In this work we have derived analytical expressions that show how the visibility of rain is affected by factors such as camera parameters, properties of rain, and the brightness of scene. We have shown that the strong dependence of the visibility of rain on camera parameters can be exploited to provide a simple and effective method to reduce/remove the effects of rain during image acquisition. The experiments demonstrate the effectiveness of our method in various common scenarios. However, this method is not as effective in reducing rain from scenes with very heavy rain or scenes with fast-moving objects that are close to the camera. In such cases post-processing [1] might be required to remove its effects. We also demonstrated how the visibility of rain can be enhanced to build an inexpensive and portable camera-based rain gauge that provides instantaneous rain rate. Enhancing or reducing the effects of rain can also be used in movies for controlling the visual effects of rain. We believe that our work has strong implications for outdoor vision systems. We are currently working on implementing a system that makes use of the results presented in [1] to automatically detect rain and then sets optimal camera parameters for reducing/removing the visibility of rain.

References

- [1] K. Garg and S.K. Nayar. Detection and removal of rain in videos. In *CVPR04*, 2004.
- [2] K. Garg and S.K. Nayar. Rain and visibility. *Technical Report*, 2005.
- [3] R. Gunn and G.D. Kinzer. Terminal velocity for water droplet in stagnant air. *J. of Hydro. Eng.*, 6:243–248, 1949.
- [4] E. Habib, W.F. Krajewski, and A. Kruger. Sampling errors of tipping-bucket rain gauge measurements. *J. of Hydro. Eng.*, 6:159, 2001.
- [5] B.K.P. Horn. *Robot Vision*. The MIT Press, 1986.
- [6] M. Löffler-Mang and J. Joss. An optical disdrometer for measuring size and velocity of hydrometeors. *J. Atmos. Ocean. Tech.*, 17:130–139, 2000.
- [7] R.M. Manning. *Stochastic Electromagnetic Image Propagation*. McGraw-Hill, Inc, 1993.
- [8] B.J Mason. *Clouds, Rain and Rainmaking*. Cambridge Press, 1975.
- [9] S.G. Narasimhan and S.K. Nayar. Vision and the atmosphere. *IJCV*, 48(3):233–254, August 2002.
- [10] S.K. Nayar and S.G. Narasimhan. Vision in bad weather. *Proceedings of the 7th International Conference on Computer Vision*, 1999.
- [11] J.P. Oakley and B.L. Satherley. Improving image quality in poor visibility conditions using a physical model for degradation. *IEEE Trans. on Image Processing*, 7, February 1998.
- [12] M. Schonhuber, H. Urban, J. P. Baptista, W. Randeu, and W. Rielder. Measurements of precipitation characteristics by a new disdrometer. *Proc. Atmos. Phys. and Dyn. in the Analysis and Prognosis of Precipitation Fields*, 1994.
- [13] K. Tan and J.P. Oakley. Enhancement of color images in poor visibility conditions. *ICIP*, 2, September 2000.
- [14] T. Wang and R.S Clifford. Use of rainfall-induced optical scintillations to measure path-averaged rain parameters. *JOSA*, 8:927–937, 1975.

6 Appendix

6.1 Exposure Time

Drops at a distance $z > z_m$ only occlude a fraction $A = \pi \left(\frac{f a}{z}\right)^2$ of pixel area (in pixels). Here a is the radius of the drop, f is the focal length (in pixels) and z is the distance of the drop from the camera. The time τ that these drops lies within the field of view of a pixel is given by $\tau = \frac{1}{v_i} \ll T$, where $v_i = f v / z$ is the image velocity of the raindrop in pixels. The intensity I_r at a pixel due to a raindrop is obtained by integrating the irradiance at the pixel over the exposure time. That is

$$\begin{aligned} I_r &= k \frac{\pi}{4 N^2} \int_0^\tau L(t) dt + \int_\tau^T L(t) dt \\ &= k \frac{\pi}{4 N^2} (\tau A L_r + \tau (1 - A) L_b + (T - \tau) L_b) \end{aligned} \quad (14)$$

Substituting for A , τ , k in terms of k_0 (see equation 2) and subtracting I_b , we get equation (4).

6.2 Variance due to a Layer of Rain

Let us look at the intensity fluctuations produced by a thin layer of rain of thickness dz (see Figure 4). These fluctuations are produced due to a change in the number of drops that a pixel sees over the duration of a frame (i.e exposure time). The probability $P(k)$ that k number of drops exist in a volume is given by a Poisson distribution [7],

$$P(k) = e^{-\bar{n}} \frac{(\bar{n})^k}{k!}, \quad (15)$$

where, $\bar{n} = \rho V$ is the mean number of drops in a given volume V and ρ is the density of rain. The volume that a pixel samples during

the exposure time is⁸ $V \approx \frac{z}{f} v T dz$, where v is the velocity of the raindrop and T is the exposure time of the camera. Substituting the value of V in the expression $\bar{n} = \rho V$, we get

$$\bar{n} = \rho (z/f) v T dz \quad (16)$$

In general, the mean number \bar{n} of drops that a pixel sees is a small fraction. Hence, the chances that two or more drops will affect a pixel during the short exposure time of a camera is very low and can be neglected⁹. Therefore, the probability P_{drop} that a pixel is affected by a drop is equal to the probability that any pixel within the width of streaks $w^d(z)$ is affected by a drop, i.e.

$$P_{drop} = P(1) w^d \simeq \bar{n} * w^d. \quad (17)$$

Hence, the variance due to a thin layer of rain is given by,

$$\begin{aligned} \sigma^2(\Delta I(z)) &= E(\Delta I(z)^2) - E(\Delta I(z))^2 \\ &= P_{drop} \Delta I(z)^2 - P_{drop}^2 \Delta I(z)^2 \end{aligned} \quad (18)$$

Since $P_{drop} \ll 1$, $P_{drop}^2 \ll P_{drop}$, and hence the second term in equation (18) can be neglected. Substituting the value of P_{drop} in the above equation we get equation (9).

6.3 Variance due to a Volume of Rain

Equation (10) can be written as,

$$\sigma_r^2(I) = k_0^2 \frac{4 a^4 \rho}{v T} (L_r - L_b)^2 \mathcal{G}(f, N, z_0), \quad (19)$$

where, $\mathcal{G}(f, N, z_0) = \int \frac{f dz}{z (w(z) + |b_c(z)|)}$. Since the integral contains $|b_c|$ we get three cases depending on the location of focus plane z_0 (Details are given in [2]).

Case 1: $z_0 > R z_m$

$$\mathcal{G}(f, N, z_0) = \frac{f z_0}{H} \ln \frac{X(z_1)}{X(2fa)} + \frac{f}{1 - \frac{H}{z_0}} \ln \frac{Y(2Rfa)}{Y(2fa)} \quad (20)$$

where, $H = \frac{f^2 p}{P}$, $X(z) = 2fa + H(1 - \frac{z_1}{z_0})$ and $Y(z) = (1 - \frac{H}{z_0})z + H$

Case 2: $z_m < z_0 < R z_m$

$$\begin{aligned} \mathcal{G}(f, N, z_0) &= \left(\frac{f z_0}{H} \ln \frac{X(z_1)}{X(2fa)} + \frac{f}{1 - \frac{H}{z_0}} \ln \frac{z_0}{Y(2fa)} \right) \dots (21) \\ &\dots + \frac{f}{1 + \frac{H}{z_0}} \ln \frac{z_0}{Y'(2fa)} \end{aligned} \quad (22)$$

where, $Y'(z) = (1 + \frac{H}{z_0})z - H$

Case 3: $z_1 < z_0 < z_m$

$$\mathcal{G}(f, N, z_0) = \frac{f z_0}{H} \ln \frac{X(z_1)}{2fa} + \frac{f z_0}{H} \ln \frac{X'(2fa)}{2fa} \dots \quad (23)$$

$$\dots + \frac{f}{1 + \frac{H}{z_0}} \ln \frac{Y'(2Rfa)}{Y'(2fa)} \quad (24)$$

where, $X'(z) = 2fa - H(1 - \frac{z_1}{z_0})$

Taking the square root we get the standard deviation due to rain as,

$$\sigma(I) = k_0 (2a)^2 \sqrt{\frac{\rho}{v T}} (L_r - L_b) \sqrt{\mathcal{G}(f, N, z_0)} \quad (25)$$

⁸The volume of this thin slice of the pyramidal section is approximately equal to $V \approx l_x l_y l_z$, where $l_x \approx \frac{z}{f}$, $l_y = v T$, and $l_z = dz$ are the lengths of its sides.

⁹The ratio $P(2)/P(1) = \bar{n}/2$, which is low as \bar{n} has a very small value.